DALTON
FULL PAPER

Studies of copper(II)-binding to bacterioferritin and its effect on iron(II) oxidation †

Suzanne Baaghil, Andrew J. Thomson, Geoffrey R. Moore and Nick E. Le Brun *

Centre for Metalloprotein Spectroscopy and Biology, School of Chemical Sciences, University of East Anglia, Norwich, UK NR4 7TJ

Received 10th August 2001, Accepted 15th October 2001
First published as an Advance Article on the web 25th January 2002

The iron-storage protein bacterioferritin (BFR) from *Escherichia coli* consists of twenty four identical subunits, each containing a dinuclear metal ion-binding site (the ferroxidase centre) at which iron(II) is oxidised to iron(III) and dioxygen is reduced. Other metal ions that are commonly found in biological systems bind to the ferroxidase centre, including manganese(II), cobalt(II) and zinc(II). In this work, copper(II)-binding to BFR and its effect on iron(II) oxidation kinetics were studied by a combination of gel filtration–copper(II) binding assay, optical, magnetic and kinetic methods. Data indicate that two copper(II) ions bind per subunit with a K_d of $\approx 2.0 \times 10^{-5}$ M and establish the order of divalent metal ion binding as Cu(II) < Co(II) < Zn(II), *i.e.* it does not follow the Irving–Williams order. A number of lower affinity copper(II)-binding sites were also detected. The presence of copper(II) was found to significantly enhance the rate of iron(II) oxidation and subsequent core formation. This effect does not arise from copper(II) bound at the ferroxidase centre but, rather, is due to displaced copper(II). The nature of the displaced copper is discussed.

Introduction

Bacterioferritin (BFR) from *Escherichia coli* is one of the best studied members of the ferritin family of iron-storage proteins.[1–7] It consists of 24 identical subunits, each of MW ≈ 18.5 kDa, that are packed together to form an approximately spherical molecule with a central cavity.[1] Large amounts of iron can be deposited as a ferric–oxy-hydroxide–phosphate mineral core within this cavity. In addition to the iron core, BFR contains up to 12 *b*-type haem groups, which are situated between symmetry-related subunit pairs, bound by two methionine residues (Met52 and Met52′)[5,8] and a dinuclear metal-binding site within each subunit,[3–5] see Fig. 1. At the latter, two divalent metal ions are bridged by two carboxylates and each has monodentate carboxylate and histidine ligands.

Studies of BFR over the past few years have revealed a great deal about the mechanism by which the protein forms an iron(III) core. Kinetic, spectroscopic, potentiometric and pH stat/oximetry studies of the wild-type protein and also site-directed variants have shown that the intra-subunit dinuclear metal-binding sites are essential for the core formation process to proceed at normal rates, and that this process occurs *via* at least three kinetically distinct phases. The fastest phase (phase 1) corresponds to the binding of two iron(II) ions at each of the dinuclear ferroxidase centres, leading to the release of two protons per metal ion (eqn. (1)).

$$2Fe^{2+} + P^z \longrightarrow [Fe_2\text{–}P]^z + 4H^+ \quad (1)$$

In the presence of oxygen, this is followed by the rapid oxidation of iron(II) to iron(III) (phase 2). The product of oxygen reduction is water rather than hydrogen peroxide,[7] which is produced at the ferritin H-chain ferroxidase centre.[9,10] Oxidation of iron(II), which is a pH-independent process (eqn. (2)), results in a likely μ-oxo-bridged iron(III) dimer at each ferroxidase centre.

$$2[Fe_2\text{–}P]^z + O_2 \longrightarrow 2[Fe_2O\text{–}P]^z \quad (2)$$

The mechanism of this process is not yet known in detail but, because the iron(II) : O_2 stoichiometry of the reaction is 4 : 1, it must involve irons at (at least) two ferroxidase centres. Two mechanistic models are currently being investigated. In the 'transient peroxide model', reaction of oxygen at one centre results in a μ-oxo-bridged iron(III) dimer and hydrogen peroxide. The latter then reacts rapidly at a second centre, giving a second μ-oxo-bridged iron(III) dimer. In the alternative 'high valent iron intermediate model', oxygen reaction at one ferroxidase centre results in a peroxo-bridged iron(III) dimer, which subsequently decays to form a μ-oxo-bridged iron(IV) dimer. This high valent intermediate then undergoes a redox-coupled reaction with a second ferroxidase centre containing iron(II), resulting in the formation of two μ-oxo-bridged iron(III) dimers. The net reaction for both schemes is that shown in eqn. (2). The involvement of two ferroxidase centres in the reduction of each oxygen molecule suggests that the functional unit of the protein may be the subunit dimer in which two ferroxidase centres are 'connected' by an inter-subunit haem group. The haem group may be involved in this mechanism, but core formation proceeds at the wild-type rate in a haem-free BFR variant.[6]

The slowest phase (phase 3) corresponds to the subsequent formation of the iron core and is only observed when more than two iron(II) ions are added per BFR subunit (*i.e.* when phase 2 is saturated). The first part of the core formation process involves core nucleation. The ferroxidase centre is required for this to occur at a normal rate and one possibility is that the proposed μ-oxo-bridged iron(III) dimer at the ferroxidase centre is able to catalyse the oxidation of additional iron(II) ions present in the protein cavity, leading to the formation of a small iron(III) cluster. A group of acidic residues located on the inside of the protein surface close to the ferroxidase centre are proposed to be important in the attachment of the nucleated core to the protein coat. Subsequent core formation may involve the continued activity of the ferroxidase centre, but for ferritins in general, it is proposed that the growing core surface

† Based on the presentation given at Dalton Discussion No. 4, 10–13th January 2002, Kloster Banz, Germany.

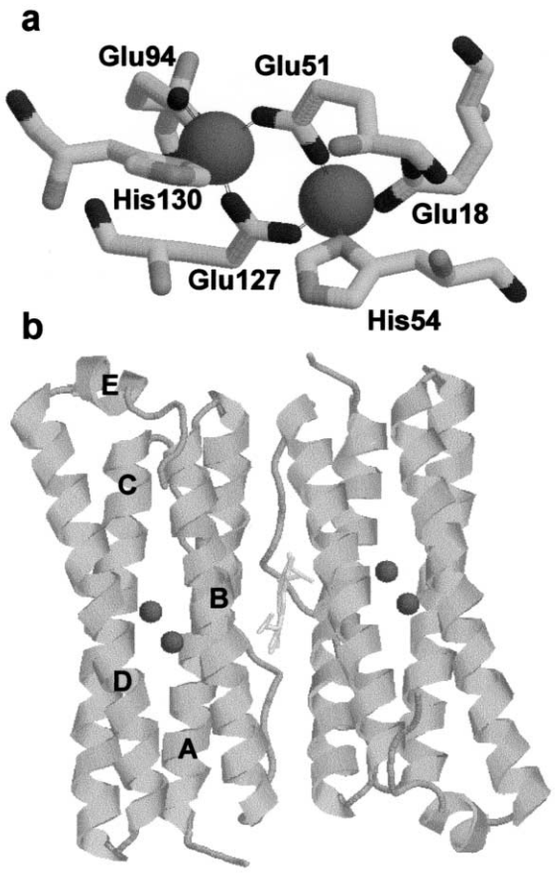

Fig. 1 The ferroxidase centre and the BFR subunit dimer. Schematic representations of (a) the dinuclear ferroxidase centre of BFR and (b) the BFR subunit dimer, showing the intra-subunit location of the ferroxidase centre and its structural relationship to the inter-subunit *b*-type haem. The ligands to the ferroxidase centre are located on helices A–D: helix A–Glu18; helix B–Glu51, His54; helix C–Glu94; helix D–Glu127, His 130. Note that the haem ligands are Met52 and Met52′. The figures were generated using Raswin (v2.6)[37] with the BFR coordinates.[5]

becomes the site of further iron(II) oxidation (the crystal growth model).[11,12]

Iron(II) is not the only divalent metal that can bind at the ferroxidase centre of BFR; cobalt(II), zinc(II) and manganese(II) are also able to do so.[1,7,13,14] Manganese(II) is most likely present at these sites in the crystalline form of BFR used in the X-ray diffraction studies of Frolow *et al*.[5] Because of its high binding affinity, zinc(II) blocks iron(II)-binding at the centre and, therefore, inhibits iron oxidation and core formation.[4] Binding of copper(II) to BFR has not been previously demonstrated, but studies of the interaction of copper(II) with mammalian ferritins have provided evidence for: high affinity binding of copper(II) to horse spleen apo-ferritin;[15] enhanced rates of iron-uptake by horse spleen ferritin containing copper(II);[16] and enhanced rates of iron-release by holo-horse spleen ferritin in the presence of copper(II),[17] suggesting that copper affects the mechanisms of iron(II) oxidation and release in ferritins. Here, we report studies of the interaction of copper(II) with BFR using a combination of UV-visible and electron paramagnetic resonance (EPR) spectroscopies, kinetic methods and metal competition experiments. We demonstrate that two copper(II) ions bind per ferroxidase centre with an affinity similar to, but less than, that of cobalt(II), and that, in contrast to cobalt(II) and iron(II), binding appears to be non-cooperative in nature. Copper(II) also binds at lower affinity protein sites. The presence of copper(II) leads to an enhanced rate of iron(II) oxidation and core formation by BFR. We show that this effect is due to copper(II) displaced from the ferroxidase centre by iron(II). The nature of the catalytic copper species is discussed.

Experimental

Overexpression of *bfr* gene and purification of wild-type BFR

Two *bfr* overexpression systems were used in the present work. In one, the *bfr* gene is expressed from its natural promoter,[6,18] while the other involved a plasmid, pGS758 (a kind gift from Dr. S. C. Andrews and Prof. J. R. Guest, University of Sheffield), in which the *bfr* gene is under control of an inducible tac promoter.[7] Expression of the *bfr* gene was induced by the addition of isopropyl ß-D-thiogalactopyranoside (IPTG) (96 mg L^{-1}) when $A_{650\ nm}$ of the growing culture (using *E. coli* JM109 as the host) was ≈ 0.15. For both systems, BFR was purified as previously described,[4] except that for the pGS758 system, the final anion exchange chromatography step was omitted.

Spectroscopic and kinetic methods

Iron oxidation measurements were made using a Hitachi U3000 spectrophotometer and optical titrations were recorded using a Hitachi U4001 spectrophotometer. Stopped-flow kinetic measurements were made using an Applied Photophysics DX17MV instrument. EPR spectra were measured with a X-band spectrometer (Bruker ER200D with an EPS 3220 computer system) fitted with an ESR9 liquid helium flow cryostat (Oxford Instruments). Copper integrations were performed using 1 mM copper(II) EDTA as a standard.

Additions of metal ions to apo-BFR

Iron(II) was added to apo-BFR as ferrous ammonium sulfate, prepared by dissolving weighed amounts of the salt in de-oxygenated AnalaR grade water. The addition of 0.25 ml concentrated HCl per 100 ml solution was found to stabilise iron(II) against autooxidation. Solutions of copper(II) chloride, cobalt(II) chloride and zinc(II) sulfate (all AnalaR grade) were prepared by dissolving weighed amounts of the salts in AnalaR grade water. Optical titrations were performed with protein solution in both sample and reference cuvettes and metal ion additions made to the sample cuvette only, while an equivalent volume of water was added to the reference. Additions were made until no further changes in the spectrum were apparent. Microlitre additions of metal ion solutions were made using a micro-syringe (Hamilton).

Other methods

Protein concentrations were determined using the bicinchoninic acid method with bovine serum albumin as a standard.[19] Haem contents were determined using the pyridine hemochromogen method of Falk[20] and were found to be 8.5 and 1.3 per 24mer for wild-type BFR (first and second expression system, respectively). Iron was removed from BFR by reduction with sodium dithionite and complexation with 2,2′-bipyridyl.[21]

The copper-binding assay was performed as follows: Following the addition of copper(II) ions to apo-BFR in 0.1 M 2-(*N*-morpholino)ethanesulfonic acid (MES) buffer, pH 6.5, and a short incubation period, the solution was applied to a small, disposable gel filtration column (PD10 column, Amersham Pharmacia Biotech) previously equilibrated in the same buffer. The protein solution was eluted from the column using the same buffer and assayed for copper using a procedure modified from Brenner and Harris.[22] Briefly, 0.75 ml of the unknown sample was mixed with 0.25 ml of trichloroacetic acid (30% w/v), vortexed and centrifuged at 13,000 rpm for 5 minutes. 0.5 ml of the supernatant was removed to a new tube and 0.1 ml of 2 mM ascorbic acid and 0.4 ml of 0.6% (w/v) bicinchoninic acid solution added, with mixing. Colour formation was measured spectrophotometrically at 562 nm. The copper concentration was determined by plotting the

$A_{562\ nm}$ reading on a calibration curve prepared using a set of copper(II) standards.

Results

Copper(II)-binding to wild-type apo-BFR

Detection of two types of binding sites. Copper(II)-binding to apo-BFR was investigated by assaying for copper(II) after the addition of 0, 10, 20, 25, 40, 50, 60, 70, 80, 90 and 100 copper(II) ions per apo-BFR molecule, and passage of the resulting solution down a gel filtration column (Experimental). A plot of copper(II) ions detected per BFR molecule as a function of copper(II) ions added per BFR molecule is shown in Fig. 2a. The

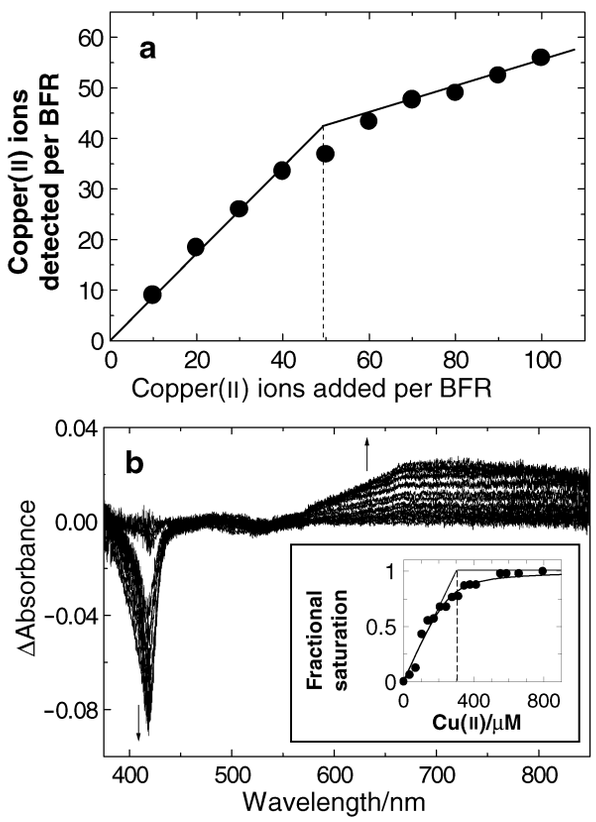

Fig. 2 Studies of copper-binding to apo-BFR. (a) Plot of copper detected per BFR *versus* copper added per BFR following passage of the BFR sample down a gel filtration column. BFR (2.0 μM) was in 100 mM MES buffer, pH 6.5. Gel filtration and copper analysis were performed as described in the Experimental. (b) UV-visible absorbance difference measurements recorded after the addition of 0, 5, 10, 15, 20, 25, 30, 35, 40, 45, 50, 55, 60, 80, 85, 95 and 115 copper(II) ions per BFR molecule, as described in the Experimental. Apo-BFR (6.9 μM) was in 100 mM MES buffer, pH 6.5. Pathlength 1 cm. Inset, plot of absorbance changes at 418 nm (expressed as a fractional saturation) as a function of copper(II) concentration. A binding curve, generated by fitting the data using an expression describing simple binding,[13] is drawn in. Arrows indicate the trends in band absorption during the titration.

plot consists of two clearly distinct phases. The first is relatively steep and corresponds to copper(II) bound tightly at specific sites in the protein coat. The second is significantly more shallow and corresponds to weaker binding of copper(II). The intersection of the two phases of the plot occurs at an added copper(II) to BFR ratio of approximately 50, suggesting that two copper(II) ions bind relatively tightly per BFR subunit. The amount of detected copper is consistently less than that added. This is because the association constant for the copper(II)–BFR complex is not infinitely high and, after the addition of copper(II) to apo-BFR, an equilibrium between bound and unbound copper is reached. Removal of unbound (or weakly bound) copper(II) by gel filtration disrupts the established equilibrium, leading to dissociation of some copper(II) as equilibrium is re-established. Hence, when the protein-bound copper(II) is collected from the column and assayed, it is always found to be lower than the copper(II) added.

Two types of copper(II)-binding to apo-BFR were also detected using UV-visible difference spectroscopy. Fig. 2b shows visible difference absorption spectra recorded during a titration of apo-BFR with copper(II) ions. As additions of copper(II) are made to the protein, difference absorption bands develop in the 400–450 nm and >650 nm regions of the spectrum. The latter are due to copper(II) d–d absorption bands. In aqueous solution, under the conditions of concentration employed here, copper(II) occurs as $[Cu(H_2O)_6]^{2+}$ or $[Cu(H_2O)_5]^{2+}$, as recently proposed by Pasquarello *et al.*[23] The extinction coefficient for aqueous copper(II) d–d absorption bands is very low ($\varepsilon_{800\ nm} \approx 10\ M^{-1}\ cm^{-1}$). The growing copper(II) d–d absorption intensity observed during the titration has a maximum shifted to ≈700 nm and is indicative of a significant increase in the copper(II) d–d extinction coefficient ($\varepsilon_{700\ nm} \approx 40\ M^{-1}\ cm^{-1}$). This is due to copper(II)-binding to the protein. This effect is expected for a transition metal ion moving from an environment of high symmetry with a centre of inversion (*i.e.* octahedral) to an environment of lower symmetry without a centre of inversion (a protein associated site).[24] The difference absorption between 400 and 450 nm is assigned to a perturbation of the BFR haem absorption upon binding of copper(II) at a site (or sites) nearby. The most significant feature of the perturbation is a negative difference band at 418 nm (which corresponds to the maximum of the Soret band), consistent with changes in intensity of the Soret band upon binding of copper(II) at a site (or sites) nearby. A similar amplitude perturbation of the haem Soret absorption has been observed previously, by stopped-flow spectrophotometry, upon binding of iron(II), zinc(II) and cobalt(II) to apo-BFR.[3,4,13] In these cases, the data were consistent with a small (<1 nm) blue shift of the Soret band upon metal ion binding. The form of the perturbation detected here is somewhat different as no positive difference absorption is observed. The reason for this is unknown, but could be due to the fact that these data are equilibrium measurements, whereas previous investigations were focused on the system prior to an equilibrium being established. The haem perturbation measured at 418 nm is plotted, in the form of fractional saturation, as a function of copper(II) ions added, see the inset of Fig. 2b. Though the data are relatively noisy, the curve fitting procedure which employs an equation describing the simplest instance of ligand binding to a protein site and which does not require that free metal ion concentration is known,[13,25] gives an intersection of the initial slope with the saturation point at ≈300 μM copper(II), which under the conditions of concentration employed here, gives an estimate of the stoichiometry of binding to be ≈44 copper(II) ions per 24mer, or ≈2 per subunit. The fit gives an average value for K_d of $2 \pm 0.6 \times 10^{-5}$ M, where the relatively large error is indicative of the noisy data set. A plot of absorption at 700 nm as a function of copper(II) ions added did not show saturation at a level of two copper(II) ions per subunit (data not shown). This suggests that, in addition to binding at the ferroxidase centre, copper(II) also binds at other, lower affinity sites. While the haem perturbation reports on copper(II) ions binding only at the ferroxidase centre, the d–d absorption bands report on copper(II) binding at all possible sites and thus do not allow clear discrimination between copper(II) bound at the high affinity site where it perturbs the haem absorbance and lower affinity sites. The data at 700 nm are consistent with the copper binding assay, which indicated copper-binding beyond a level of two per subunit. Note that at copper loadings much greater than described here, rapid precipitation of the protein occurs.

Copper(II)-binding to BFR is non-cooperative. The low temperature (30 K) EPR spectrum of apo-BFR was measured following the addition of 48 copper(II) ions per protein, Fig. 3.

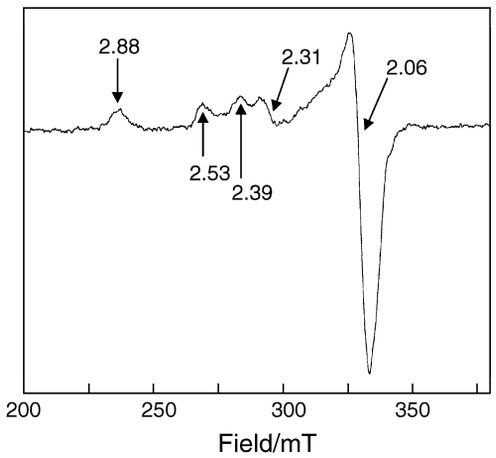

Fig. 3 EPR spectrum of BFR following addition of 48 copper(II) ions per protein. BFR was 18 μM in 0.1 M MES, pH 6.5. Measurement conditions: microwave power 2 mW, modulation amplitude 10 G, microwave frequency 9.52 GHz, temperature 30 K.

The spectrum contains signals at $g = 2.88$ and 2.31, which are due to the $S = 1/2$ low spin haem groups of BFR, and signals at $g_{\|} = 2.53$, 2.39 and $g_{\perp} = 2.06$, which arise from $S = 1/2$ copper(II). The splitting of the $g_{\|}$ signal ($A_{\|} = 149$ G) is due to interaction with the $I = 3/2$ copper nucleus. This is expected to give four hyperfine signals; two of these are not clearly resolved. Double integration of the copper(II) signals and comparison with a copper(II) integration standard revealed that only 35 ± 5% of the copper(II) is observed. Similar measurements for the addition of 24 copper(II) ions per BFR showed that only 55 ± 5% of the copper is detected. These measurements indicate that not all of the copper is present as mononuclear species, *i.e.* that magnetic coupling between closely lying copper(II) ions results in an even spin system and consequent loss of EPR intensity at $g \approx 2$. This is consistent with copper(II) binding at the dinuclear ferroxidase centre of BFR, as demonstrated for other divalent metal ions such as zinc(II) and cobalt(II).[13] However, in contrast to cobalt(II) and zinc(II), binding appears to be non-cooperative. This is concluded from a simple statistical analysis (which assumes an infinitely high binding constant) of the relative occupancy of two non-interacting sites at a dinuclear centre by single ions and by pairs of ions.[13] In the absence of cooperativity (positive or negative), addition of 24 ions per molecule (*i.e.* one per dinuclear centre) results in 12 singly occupied centres. This situation results, for a $S = 1/2$ ion such as copper(II), in an EPR signal intensity corresponding to 50% of that observed for the same concentration of mononuclear ions in solution. By the same analysis, the addition of 48 metal ions would result in 24 doubly occupied dinuclear centres, irrespective of the presence or absence of cooperativity. This would result in little or no EPR intensity at $g = 2$, depending on the nature of the magnetic coupling between the two ions at the centre. As noted above, addition of 24 and 48 copper(II) ions results in 55% and 35% mononuclear EPR intensity, figures that are higher than those predicted in the analysis. This is because the binding constant is not infinitely high. From the optical studies described above, the K_d for copper(II) binding is estimated to be $\approx 2 \times 10^{-5}$ M which, for a copper(II) concentration corresponding to 24 ions per BFR molecule, translates to binding of ≈21 of the copper(II) ions at high affinity sites. The remaining copper(II) is likely to be bound at the lower affinity sites on the protein (detected by optical experiments), with a small proportion of copper(II) in solution. In the absence of cooperativity, the 21 bound copper(II) ions are distributed randomly and, from the statistical analysis described above,[13] close to 12 dinuclear centres are predicted to be singly occupied, each giving rise to mononuclear copper(II) EPR intensity. This together with the ≈3 copper(II) ions that are not bound at the dinuclear sites gives a total of 15 mononuclear copper(II) ions, *i.e.* ≈62.5% of the total copper(II) added. Similarly, for a copper concentration corresponding to 48 per BFR molecule, taking the binding affinity into account indicates that ≈38 copper(II) ions are bound at high affinity dinuclear sites. Again, assuming no cooperativity and using the same statistical analysis, we predict a total of 8 singly occupied dinuclear centres, *i.e.* mononuclear copper(II) ions. Together with the ≈10 copper(II) ions bound elsewhere or in solution, this gives a total of 18 mononuclear copper(II) ions, *i.e.* ≈37.5% of the total copper(II) added. Both figures (62.5% and 37.5%) are, therefore, in good agreement with the EPR data (55 ± 5% and 35 ± 5%, respectively).

Relative affinities of cobalt(II), copper(II) and zinc(II) for BFR. Previous spectroscopic studies of cobalt(II)-binding to apo-BFR indicated that two cobalt(II) ions bind per dinuclear centre with an average dissociation constant of $\approx 1 \times 10^{-5}$ M. The apo-BFR titration with copper(II) ions described above yielded an estimate of the dissociation constant for the copper(II)–BFR interaction of $\approx 2.0 \times 10^{-5}$ M; *i.e.* cobalt(II) binds approximately twice as tightly as copper(II). In order to make a direct comparison of the relative affinities of these two metal ions, a competition experiment was performed using absorbance spectroscopy to follow binding processes. A sample of apo-BFR was titrated with cobalt(II) ions up to a stoichiometry of 50 cobalt(II) ions per BFR molecule (Fig. 4a). The wavelength range of the spectrum was increased compared to that reported previously[13,14] to allow perturbation of the haem absorption to be observed upon titration with cobalt(II) ions. The amplitude of the perturbation is, however, less than that observed with copper(II). This sample was subsequently titrated with aliquots of a copper(II) solution, up to a stoichiometry of 110 copper(II) ions per BFR. The resulting changes in absorption are shown in Fig. 4b. Upon addition of copper(II), the positive band with a maximum at 555 nm due to cobalt(II) d–d transitions, decreases in intensity, concomitant with an increase in intensity at higher wavelength, due to copper(II) d–d bands. An isosbestic point is observed at ≈600 nm, which allows the conversion from the wholly cobalt(II)-containing BFR to a BFR species containing copper(II) to be easily followed. In addition, the negative band at 418 nm increases further in intensity with increasing copper(II) additions. These data indicate that copper(II) displaces cobalt(II) from the dinuclear ferroxidase centres of BFR. However, because the two metal ions have similar binding affinities, complete displacement cannot be achieved under these conditions of metal ion concentration. Hence, the amplitude of the negative band at 418 nm, in the presence of 110 copper(II) ions, does not reach the amplitude observed in the copper(II)-only experiment. It is possible to calculate the relative occupancy of the ferroxidase centre sites by cobalt(II) and copper(II) at equimolar concentrations of the metal ions. Employing an extinction coefficient at 555 nm of 140 M^{-1} cm^{-1} calculated from the cobalt(II) titration data (the value is similar to the published value[13] of 155 M^{-1} cm^{-1}), the number of cobalt(II) ions bound is found to be ≈35. This indicates that ≈13 copper(II) ions occupy the remaining ferroxidase centre sites consistent with the association constants of the cobalt(II)– and copper(II)–BFR species being in the approximate ratio of 2.7 : 1. This is in reasonable agreement with dissociation constants determined by optical titration (this work and ref. 13).

In order to confirm the order of binding affinities, a similar competition experiment was performed with zinc(II) in place of cobalt(II). In this case, a perturbation of the haem Soret

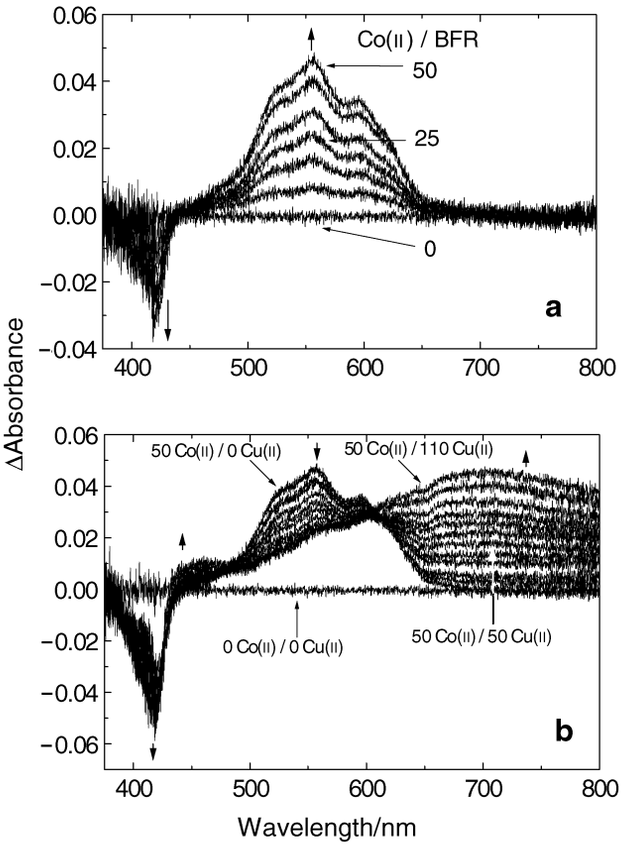

Fig. 4 Relative binding affinities of cobalt(II) and copper(II) for apo-BFR. (a) Visible absorbance difference measurements recorded after the addition of 0, 10, 20, 30, 40 and 50 cobalt(II) ions per BFR molecule, as described in the Experimental. (b) Subsequent visible absorbance difference measurements after the addition of 10, 20, 30, 40, 50, 60, 70, 80, 90, 100 and 110 copper(II) ions per BFR to BFR containing 50 cobalt(II) ions per protein. Apo-BFR (6.9 μM) was in 100 mM MES buffer, pH 6.5. Pathlength 1 cm. Arrows indicate the trends in band absorption during the titrations.

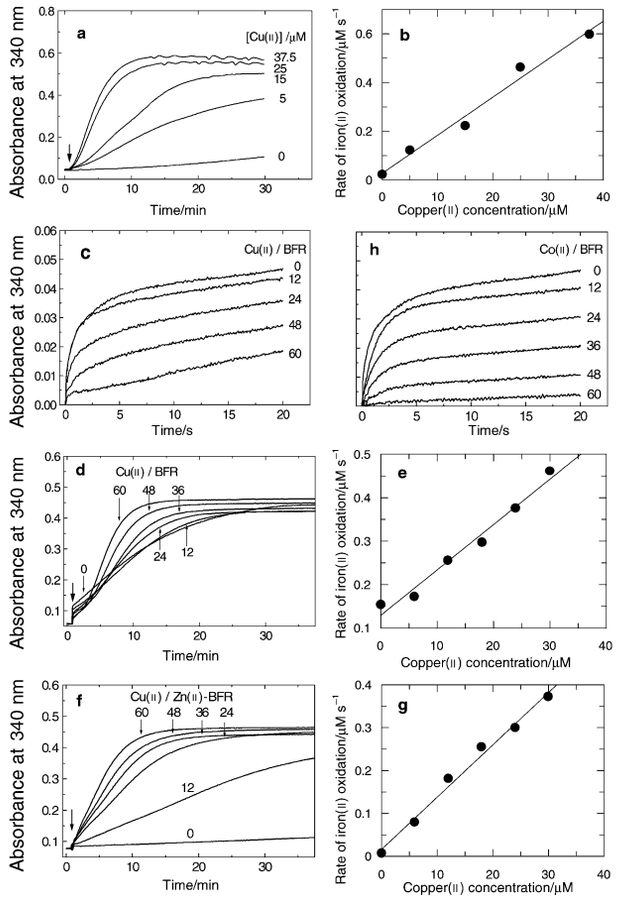

Fig. 5 Kinetic analysis of the effect of copper(II) on iron(II) oxidation catalysed by BFR. (a) Absorption changes at 340 nm as a function of time following the addition of 200 μM iron(II) to 100 mM MES buffer, pH 6.5, containing 0, 5, 15, 25 and 37.5 μM copper(II), respectively. (b) Plot of rate of iron(II) oxidation, calculated from Fig. 5a, against copper(II) concentration. (c) Phase 2 absorption changes at 340 nm as a function of time following the addition of 400 iron(II) ions per BFR containing 0, 12, 24, 36, 48 and 60 copper(II) ions per BFR molecule, respectively. (d) Phase 3 absorption changes at 340 nm as a function of time following the addition of 400 iron(II) ions per BFR containing 0, 12, 24, 36, 48 and 60 copper(II) ions per BFR molecule, respectively. (e) Plot of rate of iron(II) oxidation, calculated from Fig. 5d, against copper(II) concentration. (f) The effect of copper(II) on iron(II) oxidation catalysed by BFR containing 48 zinc(II) ions per BFR. Absorption changes at 340 nm measured as a function of time following the addition of 400 iron(II) ions per molecule to BFR containing 48 zinc(II) ions per protein and 0, 12, 24, 48 and 60 copper(II) ions per BFR, respectively. (g) Plot of rate of iron(II) oxidation, calculated from Fig. 5f, against copper(II) concentration. (h) The effect of cobalt(II) on phase 2 of iron-uptake by apo-BFR. Absorption changes at 340 nm measured as a function of time following the addition of 400 iron(II) ions per BFR containing 0, 12, 24, 36, 48 and 60 cobalt(II) ions per BFR molecule, respectively. For (c), (d), (f) and (h) the protein (0.5 μM) was in 100 mM MES buffer, pH 6.5. For (a), (c), (d), (f) and (h) the temperature was 25 °C and the pathlength was 1 cm. For (a), (d) and (f), the large arrows indicate the point at which iron(II) additions were made.

absorption was also observed upon titration with zinc(II) (data not shown), with an amplitude similar to that observed with cobalt(II) but significantly less than that observed with copper(II). Subsequent titration of copper(II) did not result in a characteristic increase in the amplitude of the haem perturbation, but did give rise to increasing absorption at 700 nm. This indicates that copper(II) is not able to displace zinc(II) from the ferroxidase centre but is still able to bind at lower affinity sites detected in the copper(II) titration and gel-filtration analysis experiments described above. These data are in agreement with the above cobalt(II)–copper(II) experiment and previously published cobalt(II)–zinc(II) competition experiments.[14]

The effect of adding 48 cobalt(II) ions on the EPR signal intensity due to BFR containing 48 copper(II) ions was investigated. After addition of cobalt(II), detectable copper(II), as determined by double integration of the $S = 1/2$ copper(II) signal in the EPR spectrum measured at 30 K (not shown), increased from 35 ± 5% to 65 ± 5%. Thus, consistent with conclusions from optical studies, cobalt(II) is able to displace a significant proportion of the copper(II) from high affinity protein sites.

The effect of copper(II) on iron(II) oxidation

The effect of copper(II) in solution. The rate of iron(II) oxidation in 0.1 M MES buffer, pH 6.5 was monitored at 25 °C as changes in absorption at 340 nm, in the presence of 0, 5, 15, 25 and 37.5 μM copper(II), respectively (Fig. 5a). The presence of copper(II) ions in solution results in a significant enhancement of the rate of iron(II) autooxidation and is dependent on the concentration of copper(II) present. The rate of iron(II) oxidation in the steady state region of the oxidation profiles was calculated in terms of μM of iron(II) oxidised per second (μM s^{-1}). A plot of the rate as a function of copper(II) concentration is shown in Fig. 5b. The increase in rate of oxidation is linear with respect to copper(II) concentration and from the gradient of the plot, we obtain rate of iron(II) oxidation per second (μM s^{-1}) per copper(II) (μM^{-1}) = 0.0156 (0.0012), where standard deviation is indicated in parentheses. In each of these experiments a red-brown precipitate of iron(III) oxyhydroxide was observed to form in the cuvette and this contributes to the large absorption increases observed through light scattering

compared to the equivalent experiments in the presence of BFR (described below). The effect of copper(II) on iron oxidation has been reported previously[26] in a study which showed that iron(II) oxidation catalysed by copper(II) is second order with respect to iron(II) and is also dependent on the concentration of copper(II).

The effect of copper(II) on iron(II) oxidation catalysed by BFR. Iron(II) oxidation catalysed by BFR consists of three distinct kinetic phases[3,4] corresponding to binding of two iron(II) ions at each dinuclear ferroxidase centre (phase 1), oxidation of iron(II) to iron(III) at the ferroxidase centre with reduction of oxygen (phase 2); and nucleation and core formation in the central cavity (phase 3). Phase 3 is only observed when more than two irons per BFR subunit are added.

Fig. 5c shows the measurement at 25 °C, by stopped-flow, of the phase 2 reaction, *i.e.* changes in absorption at 340 nm in the 20 seconds following the addition of 400 iron(II) ions per BFR to protein samples containing increasing amounts of copper(II). As the number of copper(II) ions per protein increases, so the amplitude of phase 2 decreases. However, even with 60 copper(II) ions per protein, there is appreciable oxidation after 20 seconds. The effect of copper(II) on phase 3 oxidation was also measured, Fig. 5d. In the absence of copper (the trace labelled 0), phase 2 (which requires stopped-flow methods for accurate measurement, see Fig. 5c) is followed by the much slower phase 3, which reaches completion after ≈35 minutes. The addition of an increasing amount of copper(II) ions to apo-BFR prior to the addition of iron(II) resulted in a nest of traces indicating an increasingly rapid phase 3. Because the amplitude of phase 2 is increasingly reduced and phase 3 is increasingly rapid, each trace 'crosses over' the zero copper(II) control trace. The time at which this occurs becomes shorter with increasing copper concentration. The presence of phase 2 complicates the analysis but the rate of iron(II) oxidation in the steady state region of phase 3 (*i.e.* the initial slope of phase 3) can still be calculated in terms of concentration of iron(II) oxidised per second. A plot of rate as a function of copper concentration is shown in Fig. 5e. Again this is linear which allows the calculation of the rate of iron(II) oxidation per second ($\mu M\ s^{-1}$) per copper(II) (μM^{-1}) = 0.0104 (0.0008). The rate is significantly lower than that for copper(II) in solution, indicating that different processes are occurring. The final amplitude varies with the number of copper(II) ions per protein, indicating that the optical properties of the core are dependent on the copper loading. It should be noted that even at high copper(II) loading, no evidence of precipitation is observed, indicating that all of the iron(III) formed is solubilised within the protein coat.

In order to investigate further the effect of copper on core formation, consecutive additions of 400 iron(II) ions per BFR molecule were made up to a loading of 3200 per protein to a copper(II)-free BFR sample and to a BFR sample containing 48 copper(II) ions per protein, and absorbance changes at 340 nm measured. The steady state rates of iron(II) oxidation in the two samples were plotted as a function of total iron added, see Fig. 6. The plot for BFR indicates that the rate of core formation reaches a maximum at ≈1200 irons per BFR. The absolute rates of iron(II) oxidation measured for the copper(II)–BFR sample are significantly higher than those measured in the absence of copper(II), but the plot is very similar in form, with a maximum rate observed at ≈1200 irons per BFR. Thus the patterns of iron oxidation (*i.e.* core formation), but not the absolute rates, are similar in the absence and presence of copper(II), indicating that copper is involved in the core formation process. The rate profile observed here is similar to that reported for *Pseudomonas aeruginosa* BFR[27] and is consistent with a model of core formation in which the growing core surface area is important in the mechanism of iron(II) oxidation. As the cavity becomes increasingly full, the rate of iron(II) oxidation is expected to decrease along with the exposed surface area of the growing iron core.[11,28]

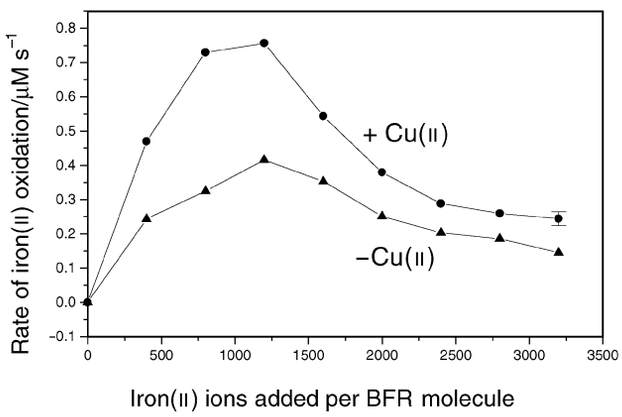

Fig. 6 Kinetic analysis of the effect of copper(II) on BFR core formation. Absorption changes at 340 nm following consecutive additions of 400 iron(II) ions per protein to BFR in the absence and presence of 48 copper(II) ion per protein were measured. Rates in the steady state region were calculated and are plotted as a function of total iron added. Filled triangles and circles represent BFR in the absence and presence of copper(II), respectively. BFR (0.5 μM) was in 100 mM MES buffer, pH 6.5, temperature was 25 °C and pathlength was 1 cm.

The effect of zinc(II) and copper(II) on iron(II) oxidation in the presence of BFR. Zinc(II) has a high affinity for the BFR ferroxidase centre ($K_d \approx 1 \times 10^{-7}$ M) and, in the presence of copper(II) (described above) and even excess iron(II),[4] remains bound at the centre. Because the ferroxidase centre is critical for the catalytic activity of the protein, the presence of zinc(II) has the effect of blocking the catalysis of iron(II) oxidation. This is shown in Fig. 5f (zero copper control trace) in which changes of absorption at 340 nm are measured after the addition of 400 iron(II) ions per BFR molecule already containing 48 zinc(II) ions. The addition of increasing amounts of copper(II) to the zinc(II)–BFR adduct prior to the addition of iron(II) resulted in the restoration of iron(II) oxidation; a phase 2 increase is not observed but the presence of copper(II) causes a significant increase in the rate of iron(II) oxidation. The rate in the steady state region for each profile was calculated and is plotted as a function of copper(II) concentration, Fig. 5g. The rates are significantly less than for copper(II) in solution and are also less than for BFR in the absence of zinc(II). This is clearly because in the absence of zinc(II), the ferroxidase activity of the dinuclear centre contributes to the rate of iron(II) oxidation. The plot is linear (as it is for both copper(II) in solution and copper(II)–BFR) and from it we can calculate the rate of iron(II) oxidation per second ($\mu M\ s^{-1}$) per copper(II) (μM^{-1}) = 0.0122 (0.0007). This is again different from that of copper(II) in solution, being closer to that measured for zinc(II)–free BFR (Fig. 5e). This indicates that the effect on the rate of oxidation per copper(II) is similar in the absence and presence of zinc(II), suggesting that the same mechanism of copper(II)-mediated catalysis is in operation in both experiments. Thus, in the presence of zinc(II), copper(II) results in ferroxidase activity which occurs *via* a mechanism that must be distinct from that involving the dinuclear ferroxidase centre.

The effect of cobalt(II) on iron(II) oxidation catalysed by BFR. Fig. 5h shows stopped flow measurements of absorption at 340 nm following the addition of 400 iron(II) ions per BFR containing increasing amounts of cobalt(II). As for the copper(II) experiment (Fig. 5c), the amplitude of phase 2 decreases with increasing cobalt(II) and is essentially abolished at a loading of 60 cobalt(II) ions per protein. In contrast to the copper experiment, however, after 20 seconds essentially no iron(II) oxidation has occurred. Measurement of BFR phase 3 iron(II) oxidation

in the presence of cobalt(II) further demonstrated a difference between copper and cobalt. Increasing amounts of cobalt(II) led to a slight but proportional decrease in the rate of phase 3 (from 0.15 μM s^{-1} in the absence of cobalt to 0.115 μM s^{-1} in the presence of 60 cobalt(II) ions per BFR) (data not shown). These data are consistent with the displacement of cobalt(II) from the ferroxidase centre by iron(II) and subsequent iron(II) oxidation and core formation.

Discussion

We have shown by gel filtration analysis, EPR spectroscopy and UV-visible difference titrations that BFR contains two distinct types of copper(II)-binding site: high affinity sites ($K_d \approx 2.0 \times 10^{-5}$ M) which are saturated at a stoichiometry of two per subunit, likely corresponding to the ferroxidase centre within each subunit; and, an uncharacterised number of lower affinity sites. Lower affinity binding sites have also been detected for zinc(II)[14] and manganese(II) (Keech, Le Brun, Mauk, Mauk, Moore and Thomson, unpublished work). The nature of these lower affinity sites are unknown, but they are likely to involve acidic residues located on the inner surface of the protein coat (*e.g.* Asp50, Asp132, Glu128 and/or Asp126), or in the hydrophilic channels connecting the exterior with the inner cavity (*e.g.* Asp109 and/or Asp118).

Competition binding studies, by difference absorption spectroscopy, show clearly (Fig. 4) that copper(II) and cobalt(II) have similar binding affinities for the ferroxidase centre, but that cobalt(II) binding is ≈2.7 times tighter. This is in agreement with independent measurements of metal binding by optical titration and is also consistent with the EPR data which shows that cobalt(II) can displace a significant proportion of copper(II) bound at the ferroxidase centre. Further interpretation of these data is not straight-forward because it is uncertain whether mixed cobalt(II)–copper(II) centres are formed. If coupled, these would be even spin and, therefore, normal-mode EPR-silent. The EPR data do show, however, that copper(II)-binding to BFR occurs non-cooperatively, in contrast to binding of cobalt(II) and zinc(II).[13] Cobalt(II) has previously been shown in a competition experiment to bind at the ferroxidase centre much less tightly than zinc(II) ($K_d \approx 1 \times 10^{-7}$ M).[13,14] Competition experiments reported here demonstrate that the order of metal ion binding affinities is copper(II) < cobalt(II) < zinc(II). This order does not follow the Irving–Williams series,[29] from which we would predict that copper(II) should form the most stable complex of all the divalent transition metal ions. This is probably because the geometries of the ferroxidase centre vary with different metal ions.

The presence of copper(II) has a marked effect on the kinetics of iron(II) oxidation (Fig. 5). Since we have demonstrated copper-binding to BFR at the ferroxidase centres of the protein, one obvious possibility is that copper(II) bound here is responsible for the observed enhancement in iron(II) oxidation activity. Experiments described above, and summarised below, show that this is not the case:

(1) The presence of cobalt(II) leads to the loss of a distinct phase 2 of BFR-catalysed iron(II) oxidation (Fig. 5h), but only a small lag in the overall rate of oxidation. Thus, it is concluded that cobalt(II) is readily displaced from the ferroxidase centre by excess iron(II). If displacement did not occur, then the rate of iron(II) oxidation would be negligible, as observed for zinc(II) (Fig. 5f, ref. 4). Given the relative affinities of copper(II) and cobalt(II), copper(II) must also be displaced from the ferroxidase centre by an excess of iron(II);

(2) The effect of copper(II) on BFR-catalysed iron(II) oxidation does not occur immediately upon addition of iron(II) (Fig. 5d); a lag is observed, consistent with the displacement of copper from the site of original binding prior to copper(II) becoming catalytic;

(3) In the zinc(II)/copper(II)/iron(II) experiment reported here (Fig. 5f), zinc(II) is added first and cannot be displaced by either iron(II) or copper(II). Hence, the observed restoration of ferroxidase activity after the addition of copper(II) ions must be due to the activity of copper(II) located elsewhere;

(4) The analysis of iron(II) oxidation rates shows that the effect of copper on the rate of oxidation is similar whether the ferroxidase centres are 'blocked' with zinc(II) or not (Figs. 5e and g). The additional contribution of the ferroxidase centre to the rate of oxidation is clear from the higher overall rates of oxidation observed in the absence of zinc(II), compare Figs. 5e and g.

The kinetics of metal ion displacement from the ferroxidase centre are determined by the rates of association and dissociation of the competing metal ions. For the displacement of divalent transition metals from the ferroxidase centre by iron(II), the relative magnitudes of the lag observed in iron(II) oxidation depend on the dissociation rates of the respective metal ions. If the dissociation rates are very high, then we might not expect to see a lag at all. In the cases of cobalt(II), described above, the effect is small but significant; in the case of zinc(II), the effect is large, *i.e.* the lag is very long because iron(II) cannot displace zinc(II) from the ferroxidase centres. Thus, zinc(II) must have a very low dissociation rate. Although the case of copper(II) is complicated by the catalytic activity of the metal ion towards iron(II) oxidation, that a lag is observed indicates that the dissociation rate of copper(II) at the ferroxidase centre is relatively low, probably being similar to cobalt(II) and much higher than zinc(II).

Once displaced from the ferroxidase centre, copper(II) is able to catalyse the oxidation of iron(II), leading to an enhancement of the rate of core formation. This raises the question of what the chemical nature of the displaced, catalytically active copper(II) is. Three possibilities are immediately apparent: (1) catalytic copper(II) is bound at the lower affinity BFR sites shown to be present in this work; (2) catalytic copper(II) is in solution; and, (3) catalytic copper(II) is in solution within the central cavity of BFR. Several observations are relevant to this issue:

(1) The kinetic characteristics of copper(II)-catalysed iron(II) oxidation in the absence (Figs. 5a and b) and presence (Figs. 5d–g) of BFR are significantly different (the rate of iron(II) oxidation per unit copper concentration decreases by a third in the presence of BFR);

(2) Iron(II) oxidation in solution results in iron(III) precipitation (Fig. 5a), but in the copper(II)/iron(II)–BFR and zinc(II)/copper(II)/iron(II) experiments reported here, iron(III) precipitation is not observed, and we conclude that the oxidised iron is solubilised within the protein coat;

(3) The effect of copper(II) on the whole process of core formation (Fig. 6) indicates that it is intimately associated with this process, *i.e.* copper(II) increases the rate of core formation but does not affect the way in which the rate depends on the state of core loading; as the BFR cavity becomes filled, the rate of iron(II) oxidation decreases similarly in the presence and absence of copper(II). The catalytic activity of copper(II) in solution would not be expected to be dependent on the state of BFR core loading.

Hence, we favour the view that copper(II) remains associated with the protein after displacement from the ferroxidase centre, either at low affinity sites or in solution in the protein cavity. We cannot rule out that some copper(II) is in solution outside the central cavity and that this contributes to the observed enhancement effect. If this contribution were to be in any way significant, it would implicate an efficient mechanism for the transfer of iron(III) into the protein cavity, because no iron precipitation is observed in the presence of BFR. Studies of mammalian ferritins have shown that transfer of iron(III) from one protein molecule to another can occur, although the period over which transfer was monitored was of the order of hours rather than minutes,[30,31] making direct comparison difficult.

The mechanism of the observed catalysis is unknown but must be associated with the ability of copper to redox cycle between +2 and +1 oxidation states. For example, the copper(II) species could oxidise iron(II) to iron(III), itself becoming reduced to copper(I) which would then be reoxidised by dioxygen, with the product copper(II) ready for reaction with another iron(II). One effect of having a copper coordination sphere dominated by oxygen (as must be the case for copper in aqueous solution which displays an even greater capacity to oxidise iron(II) than copper associated with BFR) would be to decrease the redox potential of the copper(II)/copper(I) couple,[32] favouring oxidation by dioxygen, but not to the extent that it would abolish reduction by iron(II). Cobalt is unable to react in this way because, although cobalt is also a redox active metal, cycling between its common +3 and +2 states does not occur readily because the redox potential for this couple is too high.

Does copper-binding to ferritins have any physiological relevance? A clear link has now been established in eukaryotic organisms between iron and copper metabolisms.[33–35] Whether ferritins are involved in this remains to be established, but it is noteworthy that preparations of mammalian ferritins and, to a lesser extent bacterioferritins, in our hands often contain significant amounts of copper, as judged from their EPR spectra.[36]

Acknowledgements

The authors thank Drs. Jaqui Farrar and Sholeh Dobbin for the acquisition of the EPR data. This work was supported by a project grant from the Wellcome Trust, and grants from the BBSRC and EPSRC, who support the UEA Centre for Metalloprotein Spectroscopy and Biology *via* their Biomolecular Sciences Panel. N. E. L. B. thanks the Royal Society for supporting his work on metals and metal cofactors in biology and S. B. thanks her family for financial support.

References

1 N. E. Le Brun, A. J. Thomson and G. R. Moore, *Structure Bonding (Berlin)*, 1997, **88**, 103.
2 M. R. Cheesman, N. E. Le Brun, F. H. A. Kadir, A. J. Thomson, G. R. Moore, S. C. Andrews, J. R. Guest, P. M. Harrison, J. M. A. Smith and S. J. Yewdall, *Biochem. J.*, 1993, **292**, 47.
3 N. E. Le Brun, M. T. Wilson, S. C. Andrews, P. M. Harrison, J. R. Guest, A. J. Thomson and G. R. Moore, *FEBS Lett.*, 1993, **333**, 197.
4 N. E. Le Brun, S. C. Andrews, J. R. Guest, P. M. Harrison, G. R. Moore and A. J. Thomson, *Biochem. J.*, 1995, **312**, 385.
5 F. Frolow, A. J. Kalb. and J. Yariv, *Nat. Struct. Biol.*, 1994, **1**, 453.
6 S. C. Andrews, N. E. Le Brun, V. Barynin, A. J. Thomson, G. R. Moore, J. R. Guest and P. M. Harrison, *J. Biol. Chem.*, 1995, **270**, 23268.
7 X. Yang, N. E. Le Brun, A. J. Thomson, G. R. Moore and N. D. Chasteen, *Biochemistry*, 2000, **39**, 4915.
8 M. R. Cheesman, A. J. Thomson, C. Greenwood, G. R. Moore and F. H. A. Kadir, *Nature*, 1990, **346**, 771.
9 X. Yang, Y. Chen-Barrett, P. Arosio and N. D. Chasteen, *Biochemistry*, 1998, **37**, 9743.
10 G. S. Waldo and E. C. Theil, *Biochemistry*, 1993, **32**, 13262.
11 I. G. Macara, T. G. Hoy and P. M. Harrison, *Biochem. J.*, 1972, **126**, 151.
12 N. D. Chasteen, *Met. Ions Biol. Syst.*, 1998, **40**, 479.
13 A. M. Keech, N. E. Le Brun, M. T. Wilson, S. C. Andrews, G. R. Moore and A. J. Thomson, *J. Biol. Chem.*, 1997, **272**, 422.
14 N. E. Le Brun, A. M. Keech, M. R. Mauk, A. G. Mauk, S. C. Andrews, A. J. Thomson and G. R. Moore, *FEBS Lett.*, 1996, **397**, 159.
15 S. Pead, E. Durrant, B. Webb, C. Larsen, D. Heaton, J. Johnson and G. D. Watt, *J. Inorg. Biochem.*, 1995, **59**, 15.
16 J. McKnight, N. White and G. R. Moore, *J. Chem. Soc., Dalton Trans.*, 1997, 4043.
17 H. F. Bienfait and M. L. van den Briel, *Biochim. Biophys. Acta*, 1980, **631**, 507.
18 S. C. Andrews, J. B. Findlay, J. R. Guest, P. M. Harrison, J. N. Keen and J. M. Smith, *Biochim. Biophys. Acta*, 1991, **1078**, 111.
19 P. K. Smith, R. I. Krohn, G. T. Hermanson, A. K. Mallia, F. H. Gartner, M. D. Provenzano, E. K. Fujimoto, N. M. Goeke, B. J. Olson and D. C. Klenk, *Anal. Biochem.*, 1985, **150**, 76.
20 J. E. Falk, *Porphyrins and Metalloporphyrins*, Elsevier, North-Holland, Amsterdam, vol. 2, 1964, pp. 181–182.
21 E. R. Bauminger, P. M. Harrison, D. Hechel, I. Nowik and A. Treffry, *Biochim. Biophys. Acta*, 1991, **1118**, 48.
22 A. J. Brenner and E. D. Harris, *Anal. Biochem.*, 1995, **226**, 80.
23 A. Pasquarello, I. Petri, P. Salmon, O. Parisel, R. Car, É. Tóth, D. H. Powell, H. E. Fischer, L. Helm and A. E. Merbach, *Science*, 2001, **291**, 856.
24 M. Gerloch and E. C. Constable, *Transition Metal Chemistry*, VCH Publishers, New York, 1994, pp. 64–69.
25 R. J. Leatherbarrow, GraFit, (version 3.0), Erithacus Software Ltd., Staines, UK, 1992.
26 H. Tamaru, K. Sato and M. Nagayama, *Nippon Kagaku Kaishi*, 1983, **10**, 1405.
27 S. Mann, J. M. Williams, A. Treffry and P. M. Harrison, *J. Mol. Biol.*, 1987, **198**, 405.
28 G. A. Clegg, J. E. Fitton, P. M. Harrison and A. Treffry, *Prog. Biophys. Mol. Biol.*, 1980, **36**, 56.
29 R. J. P. Williams, *FEBS Lett.*, 1982, **140**, 3.
30 S. Levi, S. J. Yewdall, P. M. Harrison, P. Santambrogio, A. Cozzi, E. Rovida, A. Albertinini and P. Arosio, *Biochem. J.*, 1992, **288**, 591.
31 E. R. Bauminger, A. Treffry, A. J. Hudson, D. Hechel, N. W. Hodson, S. C. Andrews, S. Levi, I. Nowik, P. Arosio, J. R. Guest and P. M. Harrison, *Biochem. J.*, 1994, **302**, 813.
32 S. J. Lippard and J. Berg, *Principles of Bioinorganic Chemistry*, University Science Books, California, 1994, pp. 21–42.
33 C. Askwith, D. Eide, A. V. Ho, P. S. Bernard, L. Li, S. Davis-Kaplan, D. M. Sipe and J. Kaplan, *Cell*, 1994, **76**, 403.
34 R. Stearman, D. S. Yuan, Y. Yamaguchi-Iwai, R. D. Klausner and A. Dancis, *Science*, 1996, **271**, 1552.
35 K. Yoshida, K. Furihata, S. Takeda, A. Nakamura, K. Yamamoto, H. Morita, S. Hiyamuta, S. Ikeda, N. Shimuzu and N. Yanagisawa, *Nat. Genet.*, 1995, **9**, 267.
36 N. E. Le Brun, Ph.D. Thesis, University of East Anglia, 1993.
37 R. A. Sayle and E. J. Milner-White, *Trends Biochem. Sci.*, 1995, **20**, 374.